Band mapping in the one-step photoemission theory: Multi-Bloch-wave structure of final states and interference effects

E. E. Krasovskii,[1] V. N. Strocov,[2] N. Barrett,[3] H. Berger,[4] W. Schattke,[1,5] and R. Claessen[6]
[1]*Institut für Theoretische Physik, Christian-Albrechts-Universität, Leibnizstrasse 15, D-24098 Kiel, Germany*
[2]*Swiss Light Source, Paul Scherrer Institute, CH-5232 Villigen PSI, Switzerland*
[3]*CEA-DSM/DRECAM-SPCSI, CEA-Saclay, 91191 Gif-sur-Yvette, France*
[4]*Institut de Physique Appliquee, EPFL, CH-1015 Lausanne, Switzerland*
[5]*Donostia International Physics Center (DIPC),* P.º *Manuel de Lardizábal, 4, 20018 Donostia-San Sebastián, Spain*
[6]*Experimentelle Physik 4, Universität Würzburg, 97074 Würzburg, Germany*
(Received 31 October 2006; published 26 January 2007)

A Bloch-waves based one-step theory of photoemission is developed within the augmented plane wave formalism. The multi-Bloch-wave structure of photoelectron initial and final states is found to manifest itself in strong interference of transition amplitudes between their Bloch components. This leads to prominent spectral features with characteristic photon energy dispersion, experimentally found for VSe_2 and $TiTe_2$. The Bloch-wave method offers a general band mapping tool indispensable in cases of strong interference and non-free-electron band structure, in which the common direct transitions analysis fails.

DOI: 10.1103/PhysRevB.75.045432 PACS number(s): 79.60.−i, 71.15.−m, 71.20.−b

I. INTRODUCTION

Angle resolved photoemission (ARPES) is an important tool to study electronic processes in solids.[1] We shall focus on the quasiparticle band structure, a key concept to characterize the electron system in crystals, though, for strongly interacting electrons more general terms as, e.g., the spectral function might be more appropriate. The experiment allows one to validate basic assumptions that underly *ab initio* methods, such as *GW* or time-dependent density functional theory (DFT).[2] The trial and error fitting of theoretical spectra to experiment is heavy and inefficient, and the natural language to analyze the observed spectra is the band structure $E(\mathbf{k})$.

A procedure of converting measured ARPES spectra into an *experimental* band structure is called band mapping. The fundamental difficulty arises because photoemission spectra are complex intensity distributions governed by electronic transitions that lack a complete specification by good quantum numbers and their selection rules. The momentum conservation perpendicular to the surface is heavily disturbed by the presence of the surface, which leads to complicated spectral shapes. The intensity distribution is determined by the transition probabilities and by the coupling of the outgoing electron wave across the surface to the vacuum state at the detector, both factors being strongly energy dependent. Reliability of an analysis critically depends on proper account of these factors,[3] which can in fact be achieved in the framework of the one-step theory of photoemission.[4]

However, the one-step theory has been rarely drawn on for band mapping, and one usually relies on a band structure plot to guess the surface perpendicular component $k_\perp$ of the photoelectron Bloch vector(s). On the most primitive level $k_\perp$ can be fixed by the detector energy assuming a free-electron parabolic dispersion of the final state within the solid.[5] When multiple scattering of the photoelectron is strong, one must calculate the outgoing wave function with a realistic crystal potential, including the surface. The calculations can be supported by a LEED experiment, (low energy electron diffraction) where the spectral structures reflect characteristic points of the unoccupied complex band structure (energy vs complex Bloch vector),[6] and their energy broadening gives information about the mean free path.[7] In both band mapping schemes the spectral peaks are assumed to point to direct transitions between the dispersion curves $E(\mathbf{k})$ of the initial and final states. This "geometric" scheme works well for moderate inelastic scattering and a simple structure of the final states, but it can entirely fail in complicated albeit rather common cases.

In this paper, we show that the direct transitions approach may be misleading when the interference of several Bloch waves forming the wave function comes into play. It may suppress a seemingly allowed transition or lead to a pronounced peak. This is illustrated by theoretical and experimental study of normal emission from VSe_2 and $TiTe_2$ layered crystals. We shall see that *ab initio* calculations within the one-step theory still make it possible to establish a unique correspondence between spectral peaks and definite bands, which justifies the concept of band mapping and fosters the use of ARPES for direct band structure analyses. A prerequisite for this is a formulation of the one-step theory of photoemission in terms of Bloch waves, which we introduce in this work.

In the one-step theory,[4] the photoelectron final state is described by the time reversed LEED state $|\Phi\rangle$, a pure state represented by *a damped wave function*:[8] the inelastic scattering is described by an imaginary part $-iV_\mathrm{i}$ added to the potential in the crystal half-space, so that $|\Phi\rangle$ is an eigenfunction of a non-Hermitian Hamiltonian with a real eigenvalue E_f—the final state energy. The term $-iV_\mathrm{i}$ causes the function $|\Phi\rangle$ to decay in space and provides the model with the desired surface sensitivity. The finite mean free path means a crystal momentum uncertainty of the final state Bloch waves, whose immediate effect is to broaden the spectral structure due to a direct transition. Below we discuss a less evident effect of interference between indirect transitions.

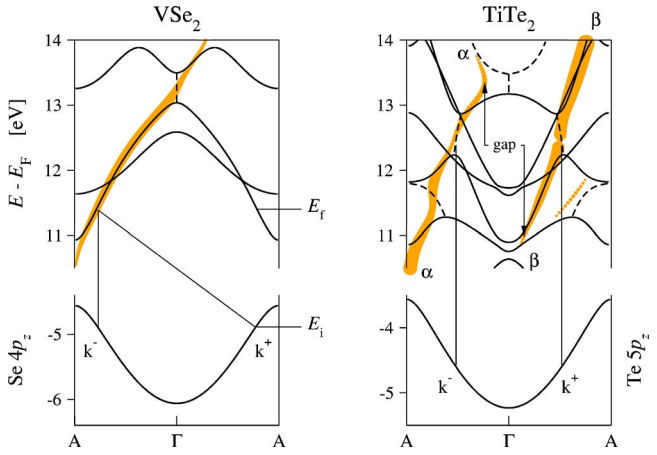

FIG. 1. (Color online) Se $4p_z$ and Te $5p_z$ bands of VSe_2 and $TiTe_2$ and some unoccupied bands. Shaded lines show the members of CBS with V_i=1 eV giving largest contributions to the $|\Phi\rangle$ state. Line thickness is proportional to the current carried (absorbed) by this partial wave (Ref. 10). Full (dashed) curves are real lines of CBS for real (complex) $k_\perp$ vectors for V_i=0 (Ref. 6). Only dashed lines related to thick lines are shown. In $TiTe_2$ two branches are important: α and β. Straight lines illustrate indirect (left panel) and direct (right) interference. Arrows in the right panel indicate the final state $k_\perp$ gap leading to the dispersion turning point in $TiTe_2$ at E_f=12.5 eV in Fig. 3.

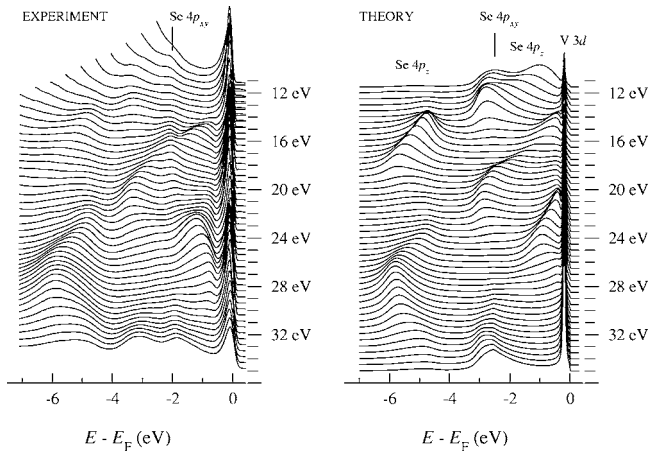

FIG. 2. Normal emission EDCs of VSe_2 parametrized by photon energy. Spectra are normalized to the same integral intensity. In calculation, initial state lifetime changes linearly from 0.05 eV at E_F to 0.75 eV at E_i=−6 eV.

The initial state is a standing wave; in the depth of the crystal it is a sum of the Bloch wave $|\mathbf{k}^+\rangle$ incident from the interior of the crystal on the surface and a number of reflected waves traveling in the opposite direction. (Apart from propagating waves, close to the surface evanescent ones contribute to the wave function.) In the simplest case there is only one reflected wave $|\mathbf{k}^-\rangle$, see Fig. 1. The dipole matrix elements $\langle\Phi|\hat{\mathbf{p}}|\mathbf{k}^+\rangle$ and $\langle\Phi|\hat{\mathbf{p}}|\mathbf{k}^-\rangle$ cancel or enhance each other depending on their phases. If the final state $|\Phi\rangle$ is a single Bloch wave, as in VSe_2 in Fig. 1, and the absorbing term V_i is small the phases of the transition amplitudes are unimportant as only the $k_\perp$-conserving transition is strong (the one at $\mathbf{k}^-$ in the left panel of Fig. 1). For realistic values of $V_i \sim 1$ eV the amplitudes become comparable. For brevity, we refer to this as *indirect* interference; its importance increases with inelastic scattering strength. If $|\Phi\rangle$ comprises several Bloch waves, as in $TiTe_2$ in Fig. 1, strong interference may occur with a negligible $k_\perp$ broadening. This we shall call *direct* interference. That the final state may comprise several Bloch waves is well known,[9] but the importance of their interference and its implications for the band mapping have not been realized.

II. RESULTS AND DISCUSSION

Computationally, we adopt the band structure approach both to final and to initial states.[11] The LEED wave function is a scattering solution for a plane wave incident from vacuum. In the bulk it is given in terms of the complex band structure (CBS), and it is continued into the surface region by solving a Cauchy problem. A detailed description of this technique for an all-electron potential of general shape within the augmented plane wave formalism has been given in Ref. 12. A special aspect of our method is that the same technique is used for initial states, only the incident wave is now the Bloch wave $|\mathbf{k}^+\rangle$. The present theory is scalar relativistic, but for $TiTe_2$ we used relativistic initial state energies and one-component scalar-relativistic wave functions. This Bloch-waves theory offers an efficient computational scheme, which takes into account the full potential in the bulk and at the surface and displays a clear connection between the spectra and the CBS of the crystal.

The ARPES experiment was performed at the SuperACO synchrotron in LURE, France. The energy distribution curves (EDCs) were measured at normal emission with photon energies between 11.5 and 35 eV. The light polarization vector was set at an angle of 45° to the surface normal in the $M\Gamma M'$ azimuth. The combined monochromator and analyzer energy resolution varied from 23 to 130 meV with increase of the photon energies through the experimental range.

Experimental and theoretical EDCs for VSe_2 are compared in Fig. 2. For both VSe_2 and $TiTe_2$ all the main structures and their dispersion with photon energy are in good agreement. Figure 3 presents a detailed analysis of the peak dispersion and reveals the accuracy limitations of the theory due to simplified treatment of quasiparticles within the local density approximation (LDA): the calculated upper Se $4p_z$ band is shifted upwards by 0.3 eV, and the Se $4p_{xy}$ band downwards by 0.5 eV.[14] Discrepancies of the same character and size are observed for the Te $5p$ states in $TiTe_2$. Although the unoccupied bands of VSe_2 are shifted by 3 to 4 eV upwards relative to the bands of $TiTe_2$ the self-energy effects are seen to start growing at roughly the same energy: below $E_f \sim 16$ eV the measured E_f location of the peaks is well reproduced, and above 16 eV the measured dispersion curves are stretched toward higher energies.

In the final state panels of Fig. 3 shaded lines show the two CBS branches giving the largest contributions to photocurrent. Naturally, the same waves effect the electron transmission in the VLEED experiment.[10] The excellent agreement between our calculated and our measured VLEED

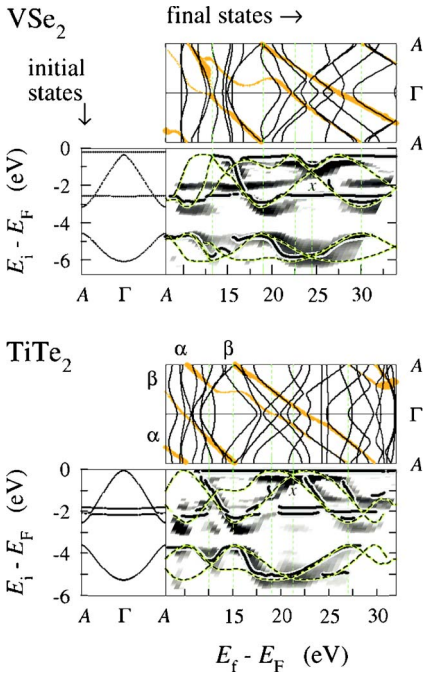

FIG. 3. (Color online) Peak dispersion diagrams $E_i(E_f)$ for normal emission from VSe_2 and $TiTe_2$. Bulk band structures for initial $E_i(k_\perp)$ and final $E_f(k_\perp)$ states are shown with thin full lines. In the final states graphs thick lines show the branches of CBS with strongest contributions to the $|\Phi\rangle$ state (thickness has the same meaning as in Fig. 1). Dashed lines show the location of direct transitions to the conducting branches of CBS (lines due to nondispersive p_{xy} and V $3d$ states are not shown). They are superimposed on full lines that show peak locations in the theoretical EDCs. In right graphs the experimental second derivative maps $-d^2I(E_i)/dE_i^2$ are shown in logarithmic colorscale [areas with $-d^2I(E_i)/dE_i^2<0$ are clipped].

spectrum for $TiTe_2$ (see Ref. 13) strengthens our confidence in the quality of the $|\Phi\rangle$ states.

The presence of two Bloch waves equally strongly contributing to the LEED function over wide energy regions not only makes the free electron model misleading but also requires that the more advanced method based on the geometry of $E_f(k_\perp)$ lines be applied with care. It is instructive to plot the direct transitions lines—a common procedure to interpret the experiment in terms of known bands: the dashed lines in Fig. 3 show the points with coordinates $[E_f(k_\perp), E_i(k_\perp)]$, with $k_\perp$ sweeping the $A\Gamma A$ interval. The theoretical peak dispersion is seen to often deviate from the direct transitions lines. A vivid example of such an intrinsic shift[15] is the downward dispersion of the lower p_z bands between 20 and 21 eV in VSe_2 and between 16 and 17 eV in $TiTe_2$.

The two-branch structure of the $|\Phi\rangle$ state also manifests itself in a curious dispersion of the lower Te $5p_z$ peak between $E_f=11$ and 15 eV: it moves downward but does not reach the band bottom and vanishes at $\sim$13 eV to appear again at the band maximum less than 3 eV higher in energy. This happens because the leading final state wave hops from branch α to branch β at $E_f \approx 12$ eV, see Fig. 1. In VSe_2 at low energies only one branch dominates, see Fig. 1, so we can more clearly see the effect: in VSe_2 the peak disperses almost to the band minimum, and the maximum is reached some 6 eV higher. The rapid change from minimum to maximum in $TiTe_2$ is caused by the $k_\perp$ gap between the α and β branches.

A constructive direct interference gives rise to the structures x in VSe_2, around $E_f=24.5$ eV at $E_i \approx -1.2$ eV, and in $TiTe_2$, around $E_f=21.5$ eV at $E_i \approx -0.5$ eV, see Fig. 3. In both cases the observed intensity enhancement correlates well with the crossing points of the two direct transition lines. In VSe_2 the structure appears well below the valence band maximum, and the $k_\perp$ vectors of both final state Bloch waves are well distant from the Γ point. In $TiTe_2$ the dispersion is less pronounced, which reflects the differences in the band structures (see right panels of Fig. 4): in $TiTe_2$ the crossing occurs much closer to the Γ point than in VSe_2, and at the same time the $E_i(k_\perp)$ dispersion is weaker. The interference origin of the features is illustrated by Fig. 4, which compares VSe_2 spectra for $\hbar\omega=25$ and 26.5 eV obtained within the one-step theory with the spectra resulting from incoherent summation of the squared moduli of the elements

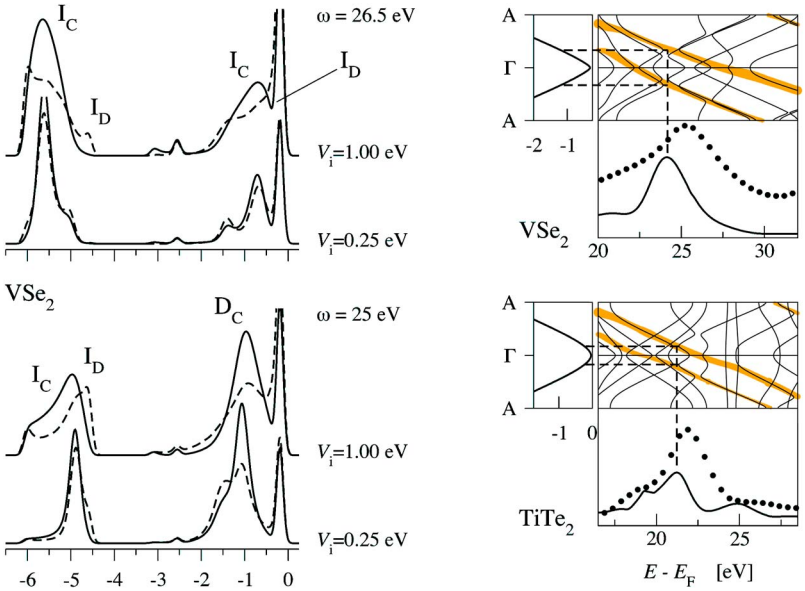

FIG. 4. (Color online) Interference effects in VSe_2. Left: Full lines are EDCs calculated within the one-step theory, and dashed lines the result of incoherent summation of the emission from the $|\mathbf{k}^-\rangle$ and $|\mathbf{k}^+\rangle$ states. Structures affected by indirect (I) and direct (D) interference are marked by symbols $I_{C,D}$ and D_C, with subscripts referring to constructive (C) and destructive (D) interference. Direct interference is recognized by its influence on the spectra with $V_i=0.25$ eV. Right: Initial and final states whose direct interference causes the feature x in the dispersion diagrams in Fig. 3. Lower panels show calculated (lines) and measured (circles) CIS spectra for the energies E_i at which the strongest intensity enhancement is observed.

$\langle\Phi|\hat{\mathbf{p}}|\mathbf{k}^{\pm}\rangle$. For a small $k_\perp$ broadening, $V_i=0.25$ eV, the deviation of a coherent curve from its incoherent counterpart reveals the effect of direct interference. The indirect interference leads to differences that are seen in $V_i=1$ eV curves and not in $V_i=0.25$ eV ones. Our important finding is that the structures *x* are due to a strong final-state energy dependence of the direct interference: in Fig. 4 the intensity enhancement D_C is large for $\hbar\omega=25$ eV and negligible for $\hbar\omega=26.5$ eV.

A higher selectivity of the direct interference transitions may reduce the ambiguity of band mapping. We illustrate this in Fig. 4; shown are constant initial state (CIS) spectra for the energies E_i at which the strongest intensity enhancement is observed. For VSe_2 the calculated and measured initial energies are $E_i=-1$ and -1.2 eV, respectively (see Fig. 2 and for $TiTe_2$ it is -0.2 and -0.5 eV. The final state energy of the direct interference transition is seen to be reliably determined in experiment (to within the expected self-energy shift). Because the *x* structure signifies a symmetric $k_\perp$ location of the two final state branches the $k_\perp$ assignment of the initial state is stable to their self-energy shift—in contrast to the case of a single-Bloch-wave final state.

III. CONCLUSIONS

To summarize, with the Bloch-waves based theory of ARPES we clearly separate out the effect of $k_\perp$ dispersion of the Bloch waves and reveal the more subtle effects of matrix elements. The measured peak dispersion in VSe_2 and $TiTe_2$ is unambiguously traced back to the band structure of initial and final states, and for the first time ARPES of these crystals is adequately described. Owing to Bloch wave interference, the knowledge of just dispersion of initial and final states is often insufficient to understand the measured spectra; naive band mapping may be misleading and should be supported by an estimate of intensities. At the same time, our results indicate a dominant role of direct transitions, so the "geometric" band mapping is justified in the absence of interference.

A special type of spectral features is discovered: they arise from the multi-Bloch-wave structure of the final states and are observed as turning points in the peak dispersion diagrams that correspond neither to minima nor to maxima of the occupied bands. They originate from the constructive interference of the amplitudes of direct transitions and, thus, provide information about the wave vectors of the final state Bloch waves.

The Bloch wave interference in the *initial* states causes the calculated peak dispersion to deviate from the direct transition lines. This effect depends upon tiny details of inelastic scattering, which is not treated *ab initio* in the one-step theory. The good agreement with experiment in cases of strong interference, thus, provides a rather direct proof in favor of the damped waves treatment of inelastic scattering.

ACKNOWLEDGMENTS

The work was supported by Deutsche Forschungsgemeinschaft via Forschergruppe FOR 353 and Grant No. CL 124/5-2, and the experiments at LURE by the EC within the Access to Research Infrastructure program.

[1] *Solid State Photoemission and Related Methods*, edited by W. Schattke and M. A. Van Hove (Wiley-VCH, Weinheim, 2003); S. Hüfner, *Photoelectron Spectroscopy* (Springer-Verlag, Berlin, 1996).

[2] G. Onida, L. Reining, and A. Rubio, Rev. Mod. Phys. **74**, 601 (2002).

[3] A. Bansil and M. Lindroos, Phys. Rev. Lett. **83**, 5154 (1999).

[4] P. J. Feibelman and D. E. Eastman, Phys. Rev. B **10**, 4932 (1974).

[5] N. V. Smith, P. Thiry, and Y. Petroff, Phys. Rev. B **47**, 15476 (1993).

[6] V. Heine, Proc. Phys. Soc. London **81**, 300 (1963).

[7] V. N. Strocov, R. Claessen, G. Nicolay, S. Hüfner, A. Kimura, A. Harasawa, S. Shin, A. Kakizaki, P. O. Nilsson, H. I. Starnberg, and P. Blaha, Phys. Rev. Lett. **81**, 004943 (1998).

[8] J. C. Slater, Phys. Rev. **51**, 840 (1937).

[9] V. N. Strocov, H. I. Starnberg, P. O. Nilsson, H. E. Brauer, and L. J. Holleboom, Phys. Rev. Lett. **79**, 467 (1997); E. Pehlke and W. Schattke, J. Phys. C **20**, 4437 (1987).

[10] The concept of absorbed currents was introduced in V. N. Strocov, H. I. Starnberg, and P. O. Nilsson, Phys. Rev. B **56**, 1717 (1997), and a detailed explanation has been presented in N. Barrett, E. E. Krasovskii, J.-M. Themlin, and V. N. Strocov, *ibid.* **71**, 035427 (2005).

[11] E. E. Krasovskii and W. Schattke, Phys. Rev. Lett. **93**, 027601 (2004).

[12] E. E. Krasovskii, Phys. Rev. B **70**, 245322 (2004).

[13] V. N. Strocov, E. E. Krasovskii, W. Schattke, N. Barrett, H. Berger, D. Schrupp, and R. Claessen, Phys. Rev. B **74**, 195125 (2006).

[14] The deviation is unexpectedly strong, however, LAPW calculations with the Ceperly-Adler form of LDA, H. E. Brauer, H. I. Starnberg, L. J. Holleboom, V. N. Strocov, and H. P. Hughes, Phys. Rev. B **58**, 10031 (1998), yield the same band energies as ours obtained with the Hedin-Lundquist potential. See also K. Terashima, T. Sato, H. Komatsu, T. Takahashi, N. Maeda, and K. Hayashi, *ibid.* **68**, 155108 (2003).

[15] V. N. Strocov, J. Electron Spectrosc. Relat. Phenom. **130**, 65 (2003).